CHALMERS

Performance Analysis of Massive MIMO in Non-Ideal Settings

NIKOLAOS KOLOMVAKIS

Signal Processing Group
Department of Signals and Systems
Chalmers University of Technology
Gothenburg, Sweden 2015

Thesis for the degree of Licentiate of Engineering

Performance Analysis of Massive MIMO in Non-Ideal Settings

Nikolaos Kolomvakis

CHALMERS

Signal Processing Group
Department of Signals and Systems
Chalmers University of Technology

Gothenburg, Sweden 2015

Kolomvakis, Nikolaos
Performance Analysis of Massive MIMO in Non-Ideal Settings.

Department of Signals and Systems
Technical Report No. R012/2015
ISSN 1403-266X

Signal Processing Group
Department of Signals and Systems
Chalmers University of Technology
SE-412 96 Göteborg, Sweden
Telephone: + 46 (0)31-722 1558
Email: nikolaos.kolomvakis@chalmers.se

This thesis has been prepared using LaTeX.

Printed by Chalmers Reproservice,
Göteborg, Sweden, November 2015.

To my family

Abstract

Recent years have witnessed an unprecedented explosion in mobile data traffic, due to the expansion of numerous types of wireless devices, which have enabled a plethora of data-hungry applications. Novel techniques, such as massive multiple-input multiple-output (MIMO) systems, represent potential candidates to support these formidable demands. However, massive MIMO systems will be a viable solution only if low-cost and energy-efficient hardware is deployed, which is particularly prone to impairments such as in-phase and quadrature-phase imbalance (IQI). Moreover, it has been theoretically shown that the benefits of massive MIMO can be reaped under Rayleigh fading conditions which is an another idealistic assumption.

In this thesis, we investigate the performance of massive MIMO systems in non-ideal hardware and channel settings. We begin with by studying the impact of IQI on massive MIMO systems. We consider both the cases whereof the receiver has perfect channel state information (CSI) and estimated CSI. Important insights are gained through the analysis of system performance indicators, such as achievable rates and channel estimation. Finally, we investigate the impact of sparse propagation channels on massive MIMO by deriving the achievable rates of linear receivers.

Paper A considers the uplink of a single-cell multi-user MIMO system with IQI. Particularly, the effect of IQI on channel estimation is investigated. Moreover, a novel pilot-based joint estimator of the augmented MIMO channel matrix and IQI coefficients is described and then, a low-complexity IQI compensation scheme is proposed which is based on the IQI coefficients' estimation and it is independent of the channel gain. The performance of the proposed compensation scheme is analytically evaluated by deriving a tractable approximation of the ergodic spectral efficiency (SE) assuming transmission over Rayleigh fading channels with large-scale fading. Finally, by deriving asymptotic power scaling laws, and proving that the SE loss due to IQI is asymptotically independent of the number of BS antennas, we show that massive MIMO is resilient to the effect of IQI.

Paper B, considers the uplink of a single-cell massive MIMO system operating in sparse channels with limited scattering. This case is of particular importance in most propagation scenarios, where the prevalent Rayleigh fading assumption becomes idealistic. We derive analytical approximations for the achievable rates of maximum-ratio combining (MRC) and zero-forcing (ZF) receivers. Furthermore, we study the asymptotic behavior of the achievable rates for both MRC and ZF receivers, when N and K go to infinity under the condition that $N/K \to c \geq 1$.

Keywords: Achievable rate, massive MIMO, IQ imbalance, sparse channels.

List of Publications

The thesis is based on part of the following papers:

[A] N. Kolomvakis, M. Matthaiou, and M. Coldrey, "IQ Imbalance in Multiuser Systems: Channel Estimation and Compensation," submitted to *IEEE Transactions on Communications*, November 2015.

[B] N. Kolomvakis, M. Matthaiou, and M. Coldrey, "Massive MIMO in Sparse Channels," in *Proc. IEEE International Symposium on Signal Processing Advances for Wireless Communications (SPAWC),* June 2014.

[C] N. Kolomvakis, M. Matthaiou, J. Li, M. Coldrey, and T. Svensson, "Massive MIMO with IQ Imbalance: Performance Analysis and Compensation," in *Proc. IEEE International Conference in Communications (ICC),* June 2015.

Acknowledgements

First of all, I would like to express my appreciation and thanks to my main supervisor and friend, Prof. Michail Matthaiou, who has been a mentor for me over the last three years. His endless patience and unconditional help constantly encourage me to mature as a researcher.

Equally important was the support and understanding I have received from my co-supervisor, Dr. Mikael Coldrey. His technical insight, encouragement and belief is a constant source of motivation.

Special thanks goes to Prof. Thomas Eriksson, for his creative inspirations and fruitful discussions during our collaboration.

Many thanks also goes to my colleagues at S2 and Ericsson, thank you all for creating a pleasant working environment. In particular, I would like to thank Prof. Tomas McKelvey for all the effort he has dedicated in making the group better and better. I would also like to thank Xinlin, not only for sharing his ideas with me but also for being a great friend.

Finally, I would like to thank my parents, as well as Aphrodite and Sophie, for their constant support, motivation and love.

This work has been supported in part by the Swedish Governmental Agency for Innovation Systems (VINNOVA) within the VINN Excellence Center Chase.

Nikolaos Kolomvakis
Göteborg, November 2015

Acronyms

3GPP:	3rd Generation Partnership Project
AWGN:	Additive White Gaussian Noise
CDF:	Cumulative Distribution Function
CSI:	Channel State Information
DCR:	Direct-Conversion Radio
LO:	Local Oscillator
LTE:	Long-term Evolution
MIMO:	Multiple-Input Multiple-Output
MMSE:	Minimum-Mean-Squared-Error
MRC:	Maximum-Ratio-Combining
PDF:	Probability Density Function
RF:	Radio Frequency
SINR:	Signal-to-Noise-plus-Interference Ratio
SNR:	Signal-to-Noise Ratio
SVD:	Singular Value Decomposition
ZF:	Zero-Forcing

Notation

$\mathbf{X}$:	Matrix $\mathbf{X}$
$\mathbf{x}$:	Vector $\mathbf{x}$
$\mathbf{X}^T$:	Transpose of matrix $\mathbf{X}$
$\mathbf{X}^H$:	Conjugate transpose of matrix $\mathbf{X}$
$\mathbf{X}^*$:	Conjugate of matrix $\mathbf{X}$
$\mathbf{X}^{-1}$:	Inverse of matrix $\mathbf{X}$
$\|\|\mathbf{X}\|\|$:	L_2 norm of matrix $\mathbf{X}$
$\det\{\mathbf{X}\}$:	Determinant of matrix $\mathbf{X}$
$\mathrm{tr}\{\mathbf{X}\}$:	Trace of matrix $\mathbf{X}$
$\mathbf{I}_N$:	$N \times N$ identity matrix
x^*:	complex conjugate of x
$\mathbb{E}\{x\}$:	expected value of x
$\mathbb{E}\{x\|y\}$:	conditional expected value of x given y
$\Re\{x\}$:	Real part of x
$\Im\{x\}$:	Imaginary part of x
$\mathcal{N}(\boldsymbol{\mu}, \boldsymbol{\Sigma})$:	Normal distribution with mean of $\boldsymbol{\mu}$ and co-variance matrix $\boldsymbol{\Sigma}$
$\mathcal{CN}(\boldsymbol{\mu}, \boldsymbol{\Sigma})$:	Complex normal distribution with mean of $\boldsymbol{\mu}$ and co-variance matrix $\boldsymbol{\Sigma}$

Contents

Part I

Overview

Chapter 1

Introduction

Data transmission over wireless networks has been increasing rapidly during the last years and it is predicted that this trend will continue also in the coming years [1]. However, physical resources will remain the same (e.g. frequencies, number of time slots). Therefore, new technologies have to be developed in order to enable this growth in the future. One of these technologies is massive multiple-input multiple-output (MIMO) systems. Massive MIMO (a.k.a. large-scale MIMO, very large MIMO) systems use antenna arrays with a few hundred antennas, simultaneously serving many tens of terminals in the same time-frequency resource. The basic premise behind massive MIMO is to reap all the benefits of conventional MIMO, but on a much greater scale.

Massive MIMO systems has emerged as one of the most promising technologies with several attractive features [2], [3]. Extra antennas help to focus energy into small regions of space to bring huge improvements in throughput compared to conventional MIMO systems, and simultaneously improve the energy efficiency [4]. Other benefits of massive MIMO include: extensive use of inexpensive low-power components, simplest linear receivers e.g, MRC, become nearly optimal [5], [6], while thermal noise, inter-cell interference and channel estimation errors vanish [7]. However, the features described above can be reaped under favorable propagation conditions, i.e., the channel vectors between different MSs should become pairwisely orthogonal as the number of antennas grow [8] and assuming that perfect hardware is deployed.

The use of low quality hardware is desirable in order to make massive MIMO an economically sustainable technological shift, or its total deployment cost will scale with the number of RF front-ends and components. Unfortunately, these low-quality RF components are more prone to hardware imperfections, such as phase noise [9] and in-phase and quadrature-phase imbalance (IQI), which refers to the mismatch between the I and Q branches, i.e., the mismatch between the real and imaginary parts of the complex signal. The latter imperfection occurs due to the limited accuracy of analogue hardware, such as finite tolerance of capacitors and transistors [10]. This leads to a degradation in the overall performance and, therefore, to a deteriorated user experience.

On a parallel avenue, measurement results [11–13] have shown that physical MIMO channels very often have a sparse multipath structure, due to insufficient richness in the

scattering environment, even for relatively small antenna dimensions [14]. This setup can occur, for instance, in macrocell urban environments where the propagation links between the users and BS are often blocked by large buildings. Although most physical channels have an underlying sparse structure, little is still known about the performance of massive MIMO systems in such propagation scenarios [15].

1.1 Aim of the Thesis

The general scope of this thesis is to analyze the realizable potential of massive MIMO in non-ideal system and channel setting. The specific thesis objectives can be summarized as follows:

- analyse the impact of IQI on channel estimation of MIMO systems;
- develop a joint estimator of the propagation MIMO channel and IQI at the receiver;
- propose a low-complexity IQI compensation scheme in order to mitigate the effect of IQI for MIMO systems;
- show that massive MIMO systems are resilient to IQI;
- analyse the performance of massive MIMO systems under a proposed parametrized channel model that captures the sparse multipath structure of the environment.

1.2 Thesis Outline

The thesis is organized as follows: In Chapter 2, we introduce the multiuser MIMO channel model, which is the basis of our theoretical analysis. In Chapter 3, we characterize the in-phase and quadrature-phase imbalance for MIMO systems. Finally, we summarize our contributions in Chapter 4.

Chapter 2

Multiuser MIMO Cellular Systems

The thesis considers the uplink performance of multiuser single-input multiple-output (MU-SIMO) systems. Therefore, in this chapter, we provide the basic background of MU-SIMO systems in terms of communication schemes, channel estimation and signal detection.

2.1 Uplink Multiuser MIMO Systems

We consider the uplink of a single-cell MU-SIMO system, which includes a BS equipped with N antennas communicating with K single-antenna mobile stations (MSs) as shown in Fig. 2.1. The $N \times 1$ received vector at the BS is

$$\mathbf{r} = \sqrt{\rho_u} \sum_{k=1}^{K} \mathbf{y}_k x_k + \mathbf{w} \tag{2.1}$$

$$= \sqrt{\rho_u} \mathbf{Y}\mathbf{x} + \mathbf{w}, \tag{2.2}$$

where $\mathbf{y}_k \in \mathrm{C}^{N\times 1}$ is the channel vector between the kth user and the BS. Moreover, $\mathbf{x}$ is a zero-mean circularly symmetric Gaussian $K \times 1$ vector (i.e. $\mathbb{E}\{\mathbf{x}\mathbf{x}^T\} = \mathbf{0}$) of independent, unit-power symbols transmitted simultaneously by the K MSs, with the average transmit power of each MS being ρ_u. Furthermore, $\mathbf{Y} \triangleq [\mathbf{y}_1, ...\mathbf{y}_K] \in \mathrm{C}^{N\times K}$ and $\mathbf{x} \triangleq [x_1, ...x_K]^T \in \mathrm{C}^{K\times 1}$. Finally, $\mathbf{w}$ is the additive white Gaussian noise (AWGN) and, without loss of generality, we assume that its elements are i.i.d Gaussian distributed with zero mean and unit variance.

More specifically, $\mathbf{Y}$ models the composite propagation channel affected by small-scale fading, geometric attenuation and log-normal shadow fading. Its elements $[\mathbf{Y}]_{nk}$ are given by

$$[\mathbf{Y}]_{nk} = [\mathbf{H}]_{nk}\sqrt{\beta_k} \tag{2.3}$$

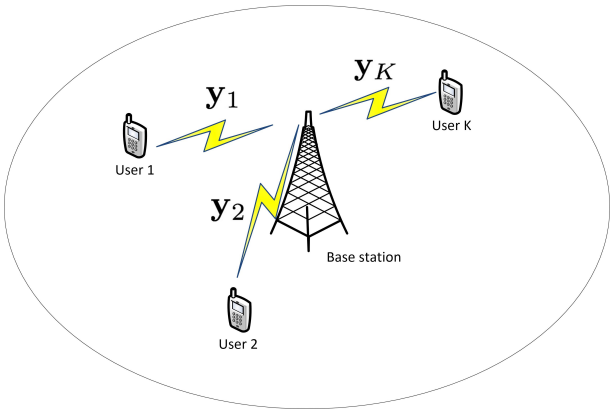

Figure 2.1: A multiuser MIMO cellular system

where $[\mathbf{H}]_{nk} \sim \mathcal{CN}(0,1)$, is the small-scale channel coefficient from the kth user to the nth antenna element. The term β_k models geometric attenuation and shadow fading between the k-th MS and BS. The large-scale fading is modeled via $\beta_k = \zeta_k / d_k^{\alpha}$, where ζ_k is the lognormal shadowing with variance σ^2. Finally, the term d_k is the reference distance between the BS and the k-th MS, and α is the path loss exponent. We can alternatively express $\mathbf{Y}$ as follows

$$\mathbf{Y} = \mathbf{H}\mathbf{D}^{1/2} \tag{2.4}$$

where $\mathbf{D}$ is a $K \times K$ diagonal matrix, whose diagonal elements are given by $[\mathbf{D}]_{kk} = \beta_k$.

The BS will coherently detect the signals transmitted from K users by using the received signal vector $\mathbf{r}$ together with the channel state information (CSI).

We assume that the channel stays constant over T symbol durations. During each coherent frame, there are two phases. In the first phase, a part τ of the coherence frame is used for uplink training to estimate the channel of each user. In the second phase, all K users simultaneously send their data to the BS. The BS then detects the transmitted symbols using the channel estimates acquired in the first phase. In the next section, we will briefly overview the principles behind channel training.

2.2 Uplink Training Phase

A part of the coherence frame is used for the uplink training. We assume that each user is assigned an orthogonal pilot sequence of τ. The pilot sequence used by the K users can be represented by a $K \times \tau$ matrix $\sqrt{\rho_p}\mathbf{S}$, which satisfies $\mathbf{S}\mathbf{S}^H = \mathbf{I}_K$, where ρ_p is the power of each pilot symbol. Then, the equivalent MIMO signal model for pilot symbol transmission at the BS is given by

$$\mathbf{R}_{\mathtt{p}} = \sqrt{\rho_p}\mathbf{Y}\mathbf{S} + \mathbf{W}_{\mathtt{p}} \tag{2.5}$$

where $\mathbf{R}_{\mathtt{p}}$ represents the $N \times \tau$ received signal matrix during pilot transmission, $\mathbf{W}_{\mathtt{p}}$ refers to the $N \times \tau$ additive noise matrix at the BS and we set the power of each pilot symbol

$\rho_p \triangleq \tau\rho_u$. Moreover, the elements of $\mathbf{W}_\mathtt{p}$ are modelled as i.i.d. Gaussian distributed with zero mean and unit variance. Assuming that $\tau \geq K$, the estimate of the channel $\mathbf{Y}$ can be obtained as

$$\widetilde{\mathbf{R}}_\mathtt{p} \triangleq \mathbf{R}_\mathtt{p}\mathbf{S}^H = \sqrt{\rho_p}\mathbf{Y} + \mathbf{N} \tag{2.6}$$

where $\mathbf{N} \triangleq \mathbf{W}_\mathtt{p}\mathbf{S}^H$ is an $N \times K$ complex complex Gaussian matrix whose elements are i.i.d. Gaussian distributed with zero mean and unit variance. Since $\mathbf{Y}$ has independent columns, we can estimate each column of $\mathbf{Y}$ independently. Let $\tilde{\mathbf{r}}_{p,k}$ and $\mathbf{n}_k$ be the kth columns of $\widetilde{\mathbf{R}}_\mathtt{p}$ and $\mathbf{N}$, respectively. Then

$$\tilde{\mathbf{r}}_{p,k} = \sqrt{\rho_p}\mathbf{y}_k + \mathbf{n}_k. \tag{2.7}$$

With Minimum Mean Square Error Estimation (MMSE), the BS estimates the channel which minimizes the mean-square error. Mathematically speaking, we have

$$\hat{\mathbf{y}}_k^* = \arg\min_{\hat{\mathbf{y}}_k \in \mathbb{C}^N} \mathbb{E}\left\{||\hat{\mathbf{y}}_k - \mathbf{y}_k||^2\right\} \tag{2.8}$$

$$= \mathbb{E}\left\{\mathbf{y}_k|\tilde{\mathbf{r}}_{p,k}\right\} = \frac{\beta_k\sqrt{\rho_p}}{\beta_k\rho_p + 1}\tilde{\mathbf{r}}_{p,k}. \tag{2.9}$$

The right hand of the expression (2.9) can be found by rewritting (2.7) as [16]

$$\sqrt{\rho_p}\mathbf{y}_k = \nu\tilde{\mathbf{r}}_{p,k} + \boldsymbol{\theta}_k \tag{2.10}$$

where $\nu = \frac{\beta_k\rho_p}{\beta_k\rho_p+1}$ and each element of $\boldsymbol{\theta}_k$ is complex Gaussian distributed variable, with zero mean and variance $\sigma^2_{\theta_k} = \frac{\beta_k\rho_p}{\beta_k\rho_p+1}$, uncorrelated with the elements of $\mathbf{y}_k$. By dividing the expression (2.10) with $\sqrt{\rho_p}$ and taking the conditional expectation we get (2.9).

2.3 Linear Receivers

For the ease of exposition, in this section we assume that the BS has perfect knowledge of the channel.[1] The BS wants to detect the transmitted signal from K users. To obtain optimal performance, the maximum-likelihood (ML) detection can be used. However, it has complexity which is exponential in the number of antennas and modulation size.

The BS can use linear detectors in order to reduce the detection complexity. However, these schemes have worse performance compared with ML. However, when the BS antennas is large, linear detectors are nearly-optimal.

2.3.1 Maximum-Ratio Combining

Maximum-Ratio Combining (MRC) maximizes the received signal-to-noise ratio (SNR) of each stream, ignoring the multiuser interference. In order to detect the transmitted

[1] In the case of imperfect CSI, any linear receiver scheme will utilize the channel estimate to recover the transmitted signal

symbol from the kth user, the received signal $\mathbf{r}$ is multiplied by the conjugate-transpose of the channel vector $\mathbf{y}_k$

$$\tilde{r}_k \triangleq \mathbf{y}_k^H \mathbf{r} = \sqrt{\rho_u}||\mathbf{y}_k||^2 x_k + \sqrt{\rho_u} \sum_{i=1, i\neq k}^{K} \mathbf{y}_k^H \mathbf{y}_i x_i + \mathbf{y}_k^H \mathbf{w}. \tag{2.11}$$

The received signal-to-interference-plus-noise ratio (SINR) of the kth stream for MRC is given by

$$\mathtt{SINR}_k^{\mathtt{mrc}} \triangleq \frac{\rho_u ||\mathbf{y}_k||^4}{\rho_u \sum_{i=1, i\neq k}^{K} |\mathbf{y}_k^H \mathbf{y}_i|^2 + ||\mathbf{y}_k||^2}. \tag{2.12}$$

The implementation of MRC is very simple since the BS multiplies the received vector with the conjugate-transpose of the channel matrix, and this can be realized in a distributed manner. Moreover, notice that for small ρ_u, $\mathrm{SINR}_k \approx \rho_u ||\mathbf{y}_k||^2$. This implies that for low SNR, MRC can achieve the same array gain as in the case of a single-user system. However, the disadvantage of MRC is that it performs poorly in interference-limited scenarios.

2.3.2 Zero-Forcing

In contrast with MRC, Zero-forcing (ZF) receivers cancel out the multiuser interference but neglecting the effect of noise. Particularly, the received vector is multiplied by the pseudo-inverse of the channel matrix $\mathbf{Y}$ as

$$\tilde{\mathbf{r}} \triangleq \left(\mathbf{Y}^H \mathbf{Y}\right)^{-1} \mathbf{Y}^H \mathbf{r} = \sqrt{\rho_u}\mathbf{x} + \left(\mathbf{Y}^H \mathbf{Y}\right)^{-1} \mathbf{Y}^H \mathbf{w}. \tag{2.13}$$

We see that the post-processing signal in (2.13) is free of multiuser interference. It is worth mentioning that this scheme requires $N \geq K$. The received SINR of the kth stream is given by

$$\mathtt{SINR}_k^{\mathtt{zf}} \triangleq \frac{\rho_u}{\left[\left(\mathbf{Y}^H \mathbf{Y}\right)^{-1}\right]_{kk}}. \tag{2.14}$$

The advantage of ZF receivers is that they can completely null out multiuser interference and their signal processing is relatively simple. However, they perform poorly under noise-limited scenarios since they boost the noise variance (a.k.a. the noise coloring effect). Moreover, ZF receivers have higher implementation complexity than MRC receivers due to the computation of the pseudo-inverse of the channel matrix.

Chapter 3

MIMO Systems with IQ Imbalance

Massive MIMO systems are built from an excessive number of antenna elements and show great promise for mobile wireless technologies. However, by increasing the number of antennas and associated radio frequency (RF) chains, the size and cost-efficiency of individual RF chains becomes more and more critical. Furthermore, a growing number of wireless standards forces for flexible solutions, which can support several communications applications.

The concept of direct-conversion radio (DCR) [17] for frequency translation is a good candidate for the massive MIMO transceiver structure. First, it is flexible and thus able to operate with several different air interfaces, frequency bands and waveforms [18]. Moreover, it does not need external intermediate frequency (IF) filters and image rejection filters [19]. Instead, the image rejection is provided by the signal processing in the in-phase (I) and quadrature (Q) arm. Therefore, this architecture opens the door to monolithic integration of the analog front-end and, thus, low-cost implementations [20].

The DCR architecture, also referred to as homodyne or zero-IF architecture, however, has some disadvantages compared to more conventionally used heterodyne architectures. These disadvantages include DC offset through self-mixing, $1/f$-noise and severe IQ mismatch [20]. This chapter will focus on the latter impairment which is caused by mutual differences in the components used for frequency translation. These differences result in a phase and/or amplitude imbalance between the I and Q signals, an effect which we will refer to as IQ imbalance.

In this chapter, we will consider the influence of IQ mismatch in both the transmitter (TX) and receiver (RX) front-ends. First, Section 3.1 introduces the homodyne transceiver structure and Section 3.2 shows the influence of IQ mismatch on the transmitted and received signals.

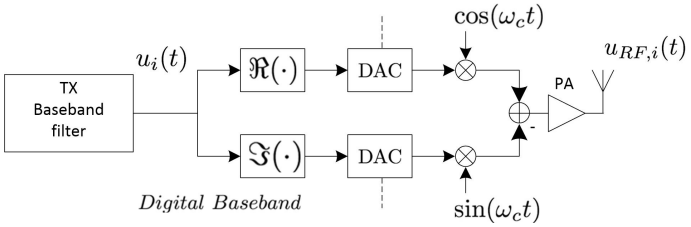

Figure 3.1: Block diagram of a homodyne transmitter [20].

3.1 Transmit/Receive front-end architecture

We first consider the up-conversion of the baseband signal $u_i(t)$ in the ith TX branch ($1 \leq i \leq N_T$, where N_T is the total number of transmit antennas), as illustrated in Fig. 3.1. The real and imaginary part of the digital baseband signal are passed through the digital-to-analog converters (DACs). The signal is then up-converted to radio frequency (RF) with carrier frequency f_c, using the quadrature mixing structure as illustrated in the figure. The RF signal pass through the power amplifier (PA), which, we will assume to be perfect with unity gain.

In case of ideal matching between the I and Q branches, the local oscillator (LO) signals that multiplies the I and Q branches differ by a 90° phase shift. Thus, they can be expressed as

$$a_Q(t) = \sin(\omega_c t), \tag{3.1}$$
$$a_I(t) = \cos(\omega_c t) \tag{3.2}$$

Using these expressions, the RF TX signal for the i-th branch can be written as

$$u_{RF,i}(t) = 2(\Re\{u_i(t)\}\cos(\omega_c t) - \Im\{u_i(t)\}\sin(\omega_c t)) \tag{3.3}$$
$$= u_i(t)e^{j\omega_c t} + u_i^*(t)e^{j\omega_c t}, \tag{3.4}$$

where $\omega = 2\pi f_c$ and where $\Re\{\cdot\}$ and $\Im\{\cdot\}$ give the real and imaginary part of their arguments. The factor 2 is added for notational convenience.

At the rth RX branch ($1 \leq r \leq N_R$, where N_R is the total number of transmit antennas), as illustrated in Fig. 3.2., the received RF signal $y_{RF,r}(t)$ is first amplified by a low-noise amplifier (LNA), which we will assume to be ideal with unity gain. Down-conversion is done again by two 90° phase shifted LO signals at RF f_c. Low-pass filtering is applied in both branches to remove higher order modulation products. Both signals are then passed through the analog-to-digital convertors (ADCs) and combined to form the baseband signal $y_r(t)$, which is input to the baseband RX filter. In the case of ideal matching between the I and Q branch, the LO signals multiplying the I and Q signal again differ by a 90° phase shift. They can be written as

$$b_Q(t) = -\sin(\omega_c t), \tag{3.5}$$
$$b_I(t) = \cos(\omega_c t). \tag{3.6}$$

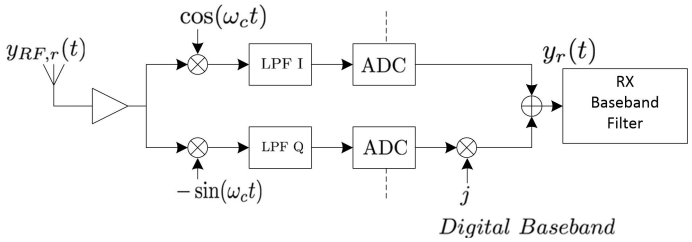

Figure 3.2: Block diagram of a homodyne receiver [20].

From (3.4) it can be concluded that the received RF signal on the rth RX branch is given by

$$y_{RF,r}(t) = y_r(t)e^{j\omega_c t} + y_r^*(t)e^{-j\omega_c t}. \tag{3.7}$$

Using (3.5), (3.6) and (3.7) the baseband RX signals are given by

$$y_r(t) = y_{I,r}(t) + jy_{Q,r}(t), \tag{3.8}$$

where, as we define LPF$\{\cdot\}$ to be the low-pass filtering operation, while

$$\begin{aligned} y_{I,r}(t) &= \text{LPF}\{b_I(t)y_{RF,r}(t)\} = \text{LPF}\{\cos(\omega_c)y_{RF,r}(t)\} && (3.9)\\ &= \frac{1}{2}\text{LPF}\{y_r(t)(1+e^{j2\omega_c t}) + y_r^*(t)(1+e^{-j2\omega_c t})\} && (3.10)\\ &= \Re\{y_r(t)\}, && (3.11) \end{aligned}$$

and

$$\begin{aligned} y_{Q,r}(t) &= \text{LPF}\{b_Q(t)y_{RF,r}(t)\} = \text{LPF}\{-\sin(\omega_c)y_{RF,r}(t)\} && (3.12)\\ &= \frac{1}{2}\text{LPF}\{y_r(t)(e^{j2\omega_c t}-1) + y_r^*(t)(1-e^{-j2\omega_c t})\} && (3.13)\\ &= \Im\{y_r(t)\}. && (3.14) \end{aligned}$$

3.2 IQ imbalance

The results in Section 3.1 show that for a system with ideal I/Q brances the baseband signals are perfectly up-converted in the TX and that the image signal centered around f_c is perfectly removed by the low-pass filters in the down-conversion. In practical systems, however, ideal matching between the I and Q branch of the quadrature TX/RX is not possible due to limited accuracy of RF front-end hardware. This will result in phase and amplitude mismatch between the I and Q branch. Several stages in the transceiver structure can contribute to the IQ mismatch, e.g., errors in the nominal 90° phase shift

between the LO signals used for up- and down-conversion of the I and Q signals and the difference in amplitude transfer of the total I and Q arms [20]. These imbalances are generally modelled as phase and/or amplitude errors in the LO signal used for up- and down-conversion. The imbalances can be modeled either symmetrical or asymmetrical. In the symmetrical method, each branch (I and Q) experiences half of the phase and amplitude errors, see e.g. [21]. In the asymmetrical method, the I branch is modeled to be ideal and the errors are modeled in the Q branch, see e.g. [22]. Nevertheless, these two methods are equivalent [20]. We will use the asymmetrical model for our analysis in this chapter. For this model the imbalanced LO signals used for up-conversion are given by

$$a_Q(t) = g_T \sin(\omega_c t + \phi_T), \tag{3.15}$$
$$a_I(t) = \cos(\omega_c t) \tag{3.16}$$

where g_T and ϕ_T model the TX gain and phase mismatch, respectively. We can conclude from (3.1) and (3.2) that for perfect matching, these imbalance parameters are given by $g_T = 1$ and $\phi_T = 0$, respectively. The TX RF signal on the ith branch can then be expressed as

$$u_{RF,i}(t) = 2(\Re\{u_i(t)\}\cos(\omega_c t)\Im\{u_i(t)\}g_T \sin(\omega_c t + \phi_T)) \tag{3.17}$$
$$= e^{j\omega_c t}\left(\Re\{u_i(t)\} + j g_T e^{j\phi_T}\Im\{u_i(t)\}\right) \tag{3.18}$$
$$+ e^{-j\omega_c t}\left(\Re\{u_i(t)\} - j g_T e^{-j\phi_T}\Im\{u_i(t)\}\right). \tag{3.19}$$

By defining the coefficients G_1 and G_2, as

$$G_1 \triangleq (1 + g_T e^{j\phi_T})/2, \tag{3.20}$$
$$G_2 \triangleq (1 - g_T e^{-j\phi_T})/2, \tag{3.21}$$

respectively, $u_{RF,i}(t)$ can be rewritten as

$$u_{RF,i}(t) = \left(G_1 u_i(t) + G_2^* u_i^*(t)\right) e^{j\omega_c t} + \left(G_1^* u_i^*(t) + G_2 u_i(t)\right) e^{-j\omega_c t}. \tag{3.22}$$

It is noted that for perfect TX matching $G_1 = 1$ and $G_2 = 0$ and that (3.22) reduces to (3.4). When we subsequently consider the imbalance on the received side, the imbalanced LO signals used for down-conversion are given by

$$b_Q(t) = -g_R \sin(\omega_c t + \phi_R), \tag{3.23}$$
$$b_I(t) = \cos(\omega_c t), \tag{3.24}$$

where g_R and ϕ_R model the RX gain and phase mismatch, respectively. Note that we can conclude from (3.5) and (3.6) that when there is ideal matching, these imbalance parameters are given by $g_R = 1$ and $\phi_R = 0$, respectively. Down-conversion of the RF

RX signal, as expressed by (3.7), then yields

$$\hat{y}_r(t) = \hat{y}_{I,r}(t) + j\hat{y}_{Q,r}(t) \tag{3.25}$$
$$= \mathrm{LPF}\{\cos(\omega_c t) y_{RF,r}(t)\} + j\mathrm{LPF}\{-g_R \sin(\omega_c t + \phi_R) y_{RF,r}(t)\} \tag{3.26}$$
$$= \Re\{y_r(t)\} + j\Im\{g_R e^{-j\phi_T} y_r(t)\} \tag{3.27}$$
$$= K_1 y_r(t) + K_2 y_r^*(t), \tag{3.28}$$

Note that the coefficients K_1 and K_2 are given by

$$K_1 \triangleq (1 + g_R e^{-j\phi_R})/2, \tag{3.29}$$
$$K_2 \triangleq (1 - g_R e^{j\phi_R})/2, \tag{3.30}$$

respectively. Again, for perfect matching we find that $K_1 = 1$ and $K_2 = 0$. For that case (3.28) reduces to (3.8).

Finally, in the context of MIMO systems, for the transmit antenna array, (3.22), can be rewritten as a $N_T \times 1$ vector

$$\mathbf{u}_{RF}(t) = \left(\mathbf{G}_1 \mathbf{u}(t) + \mathbf{G}_2^* \mathbf{u}^*(t)\right) e^{j\omega_c t} + \left(\mathbf{G}_1^* \mathbf{u}^*(t) + \mathbf{G}_2 \mathbf{u}(t)\right) e^{-j\omega_c t}. \tag{3.31}$$

where $\mathbf{u}(t) = [u_1(t), ...u_{N_T}(t)]^T$. Moreover, $\mathbf{G}_1$ and $\mathbf{G}_2$ are diagonal matrices defined as

$$\mathbf{G}_1 = (\mathbf{I} + \boldsymbol{g}_T e^{j\boldsymbol{\phi}_T})/2, \tag{3.32}$$
$$\mathbf{G}_2 = (\mathbf{I} - \boldsymbol{g}_T e^{-j\boldsymbol{\phi}_T})/2, \tag{3.33}$$

where $\mathbf{I}$ denotes the identity matrix and where

$$\boldsymbol{g}_T \triangleq \mathrm{diag}\left\{\boldsymbol{g}_{T,1}, ..., \boldsymbol{g}_{T,N_T}\right\} \tag{3.34}$$
$$\boldsymbol{\phi}_T \triangleq \mathrm{diag}\left\{\boldsymbol{\phi}_{T,1}, ..., \boldsymbol{\phi}_{T,N_T}\right\}, \tag{3.35}$$

are the diagonal matrices contain the TX amplitude and phase mismatches.

Similarly, after down-conversion with the imbalanced quadrature RX, the received baseband signal $N_R \times 1$ vector is given by

$$\hat{\mathbf{y}}(t) = \mathbf{K}_1 \mathbf{y}(t) + \mathbf{K}_2^* \mathbf{y}^*(t) \tag{3.36}$$

where $\mathbf{y}(t) = [y_1(t), ...y_{N_R}(t)]^T$ and

$$\mathbf{K}_1 = (\mathbf{I} + \boldsymbol{g}_R e^{-j\boldsymbol{\phi}_R})/2, \tag{3.37}$$
$$\mathbf{K}_2 = (\mathbf{I} - \boldsymbol{g}_R e^{j\boldsymbol{\phi}_R})/2, \tag{3.38}$$

with

$$\boldsymbol{g}_R \triangleq \mathrm{diag}\left\{\boldsymbol{g}_{R,1}, ..., \boldsymbol{g}_{R,N_T}\right\} \tag{3.39}$$
$$\boldsymbol{\phi}_R \triangleq \mathrm{diag}\left\{\boldsymbol{\phi}_{R,1}, ..., \boldsymbol{\phi}_{R,N_T}\right\}, \tag{3.40}$$

are the diagonal matrices contain the RX amplitude and phase mismatches.

Chapter 4

Contributions

This thesis consists of two main contributions. The first one investigates the impact of IQI on both conventional and massive MIMO systems. The second elaborates on the effect of sparse channels on massive MIMO systems. In Section 4.1, we list the papers that are appended to this thesis and summarize our contributions.

4.1 Included Publications

1. **Paper A: "IQ Imbalance in Multiuser Systems: Channel Estimation and Compensation"**
   In this paper, we consider the uplink of a single-cell multi-user single-input multiple-output (MU-SIMO) system with in-phase and quadrature-phase imbalance (IQI). This scenario is of particular importance, especially, in MU-SIMO systems with large antenna arrays, where the deployment of lower cost, lower-quality components is desirable to maintain their total implementation cost to affordable levels. Particularly, we investigate the effect of RX IQI on the performance of MU-SIMO systems with large antenna arrays employing maximum ratio combining (MRC) receivers. In order to study how IQI affects channel estimation, we derive a new channel estimator for the IQI-impaired model and show that IQI can downgrade the spectral efficiency (SE) of MRC receivers. Moreover, a novel pilot-based joint estimator of the augmented MIMO channel matrix and IQI coefficients is described and then, a low-complexity IQI compensation scheme is proposed which is based on the IQI coefficients estimation and it is independent of the channel gain. The performance of the proposed compensation scheme is analytically evaluated by deriving a tractable approximation of the ergodic SE assuming transmission over Rayleigh fading channels with large-scale fading. Finally, by deriving asymptotic power scaling laws, and proving that the SE loss due to IQI is asymptotically independent of the number of BS antennas, we show that massive MIMO is resilient to the effect of IQI.

2. **Paper B: "Massive MIMO in Sparse Channels"**
   Massive multi-user multiple-input multiple-output (MU-MIMO) systems are cellular

networks where the base stations (BSs) are equipped with hundreds of antennas, N, and communicate with tens of mobile stations (MSs), K, such that, $N \gg K \gg 1$. Contrary to most prior works, in this paper, we consider the uplink of a single-cell massive MIMO system operating in sparse channels with limited scattering. This case is of particular importance in most propagation scenarios, where the prevalent Rayleigh fading assumption becomes idealistic. We derive analytical approximations for the achievable rates of maximum-ratio combining (MRC) and zero-forcing (ZF) receivers. Furthermore, we study the asymptotic behavior of the achievable rates for both MRC and ZF receivers, when N and K go to infinity under the condition that $N/K \to c \geq 1$. Our results indicate that the achievable rate of MRC receivers reaches an asymptotic saturation limit, whereas the achievable rate of ZF receivers grows logarithmically with the number of MSs.

References

[1] Ericsson, "Ericsson mobility report: On the pulse of the networked society," Nov. 2014. [Online]. Available: http://www.ericsson.com/res/docs/2014/ericsson-mobility-report-november-2014.pdf

[2] F. Rusek, D. Persson, B. K. Lau, E. G. Larsson, T. L. Marzetta, O. Edfors, and F. Tufvesson, "Scaling up MIMO: Opportunities and challenges with very large arrays," *IEEE Signal Process. Mag.*, vol. 30, no. 1, pp. 40–46, Jan. 2013.

[3] T. L. Marzetta, "Noncooperative cellular wireless with unlimited numbers of base station antennas," *IEEE Trans. Wireless Commun.*, vol. 9, no. 11, pp. 3590–3600, Nov. 2010.

[4] E. G. Larsson, F. Tufvesson, O. Edfors, and T. L. Marzetta, "Massive MIMO for next generation wireless systems," *IEEE Commun. Mag.*, vol. 52, no. 2, pp. 186–195, Feb. 2014.

[5] H. Q. Ngo, E. G. Larsson, and T. L. Marzetta, "Energy and spectral efficiency of very large multiuser MIMO systems," *IEEE Trans. Commun.*, vol. 61, no. 4, pp. 1436–1449, Apr. 2013.

[6] J. Hoydis, S. ten Brink, and M. Debbah, "Massive MIMO in the UL/DL of cellular networks: How many antennas do we need?" *IEEE J. Sel. Areas Commun.*, vol. 31, no. 2, pp. 160–171, Feb. 2013.

[7] H. Yang and T. L. Marzetta, "Performance of conjugate and zero-forcing beamforming in large-scale antenna systems," *IEEE J. Sel. Areas Commun.*, vol. 31, no. 2, pp. 172–179, Feb. 2013.

[8] J. Chen, "When does asymptotic orthogonality exist for very large arays?" in *Proc. IEEE GLOBECOM*, Dec. 2013.

[9] A. Pitarokoilis, S. K. Mohammed, and E. G. Larsson, "Uplink performance of time-reversal MRC in massive MIMO systems subject to phase noise," *IEEE Trans. Wireless Commun.*, vol. 14, no. 2, pp. 711–723, Feb. 2015.

[10] A. Hakkarainen, J. Werner, K. Dandekar, and M. Valkama, "Widely-linear beamforming and RF impairment suppression in massive antenna arrays," *J. Commun. Netw.*, vol. 15, no. 4, pp. 383–397, Aug. 2013.

[11] M. Matthaiou, A. M. Sayeed, and J. A. Nossek, "Sparse multipath MIMO channels: Performance implications based on measurement data," in *Proc. IEEE SPAWC*, June 2009, pp. 364–368.

[12] L. Wood and W. S. Hodgkiss, "A reduced-rank eigenbasis MIMO channel model," in *Proc. IEEE WTS*, Apr. 2008, pp. 78–83.

[13] S. Wyne, A. Molisch, P. Almers, G. Eriksson, J. Karedal, and F. Tufvesson, "Statistical evaluation of outdoor-to-indoor office MIMO measurements at 5.2 GHz," in *Proc. IEEE VTC*, May 2005, pp. 146–150.

[14] A. M. Sayeed, "Deconstructing multiantenna fading channels," *IEEE Trans. Signal Process.*, vol. 50, no. 10, pp. 2563–2579, Oct. 2002.

[15] T. Datta and A. Chockalingam, "Increasing system capacity in uplink multiuser MIMO using sparsity exploiting receiver," in *Proc. IEEE PIMRC*, Sep. 2010.

[16] D. Gu and C. Leung, "Performance analysis of transmit diversity scheme with imperfect channel estimation," *IEE Electron. Lett.*, vol. 39, pp. 402–403, Feb. 2003.

[17] A. A. Abidi, "Direct-conversion radio transceivers for digital communications," *IEEE Journ. of Solid-State Circuits*, vol. 30, pp. 1399–1410, Dec. 1995.

[18] R. W. Chang, "Synthesis of band-limited orthogonal signals for multichannel data transmission," *Bell System Techn. Journal*, vol. 45, pp. 1775–1796, 1966.

[19] B. Razavi, "Design considerations for direct-conversion receivers," *IEEE Trans. on Circuits and Systems II: Analog and Digital Signal Processing*, vol. 44, no. 6, pp. 428–435, June 1997.

[20] T. Schenk, *RF Imperfections in High-Rate Wireless Systems: Impact and Digital Compensation*. Springer Netherlands, 2008.

[21] B. Razavi, *RF Microelectronics*. ser. Prentice-Hall Communications Engineering and Emerging Technologies Series. Prentice Hall, 1998.

[22] M. R. M. Valkama and V. Koivunen, "Advanced methods for I/Q imbalance compensation in communication receivers," *IEEE Trans. Signal Process.*, vol. 49, pp. 2335–2344, Oct. 2001.

Part II

Included papers